WEIJUAN LI*,#, SHENGSHI ZHAO*, HENGYI ZHANG**, XIAOLONG JIN***

RELATIONSHIP BETWEEN BAKE HARDENING, SNOEK-KÖSTER AND DISLOCATION-ENHANCED SNOEK PEAKS IN COARSE GRAINED LOW CARBON STEEL

In the present work, specimens prepared from coarse grained low carbon steel with different prestrains were baked and then, their bake hardening (BH) property and internal friction were determined. TEM was used to characterize the dislocation structure in BH treated samples. The measurements of internal friction in prestrained samples and baked samples were carried out using a multifunctional internal friction apparatus. The results indicate that, in coarse grained low carbon steel, the bake hardening properties (BH values) were negative, which were increased by increasing the prestrain from 2 to 5%, and then were decreased by increasing the prestrain from 5 to 10%. In the specimen with prestrain 5%, the BH value reached the maximum value and the height of Snoek-Köster peak was observed to be the maximum alike. With increasing the prestrain, both of the BH value and Snoek-Köster peak heights are similarly varied. It is concluded that Snoek-Köster and dislocation-enhanced Snoek peaks, caused by the interactions between interstitial solute carbon atoms and dislocations, can be used in further development of the bake hardening steels.

Keywords: low carbon steel, ultra-low carbon bake-hardening (ULC-BH) steel, bake hardening (BH), Snoek peak, dislocation-enhanced Snoek peak, Snoek-Köster peak, internal friction

1. Introduction

The automotive industry is one of the largest market for steel industry, consuming over 20% of steel productions [1]. Therefore, the steel industry must fully meet the requirements of the automotive industry: enhancing the fuel efficiency and reducing the vehicle mass without sacrificing current strength and stiffness of the steels. It has been shown that a 10% vehicle mass reduction leads to 6% fuel efficiency improvement [1]. The desired steel for the automotive industry is a particular combination of formability, paintability, weldability, higher strength and stiffness of a sufficient level to resist denting and buckling. These conflicting properties are desired for the steel sheets to produce the outer body panel of vehicle. Using bake hardenable steels, many conflicting properties may be achieved. The bake hardenability allows the automotive industry to use a steel with a lower flow stress of 180-250 MPa in the as-received state similar to a deep drawing grade, while after press forming and paint baking, the strength and dent resistance will be increased by 20-60 MPa in the final product, similar to a high strength steel grade [2]. The increase in strength due to the bake hardening (BH) can lead to use the thinner gauge steel sheet and thus reduce vehicle mass. In these steels, the composition is controlled so that after processing there is no free nitrogen and only a minute amount of solute carbon in ferrite (< 25 ppm). During press forming, fresh dislocations are introduced in the steel and in the subsequent paint baking treatment, the dissolution excess carbon atoms diffuse to pin free dislocations so that the strength of the produced steel panels is increased. The strength increment caused by bake hardening depends on the amount of excess solute carbon atoms in the steel. Increasing the solute carbon level increases the number of carbon atoms available to lock the dislocations but it also increases the strain aging susceptibility at room temperature. In practice, the maximum level of solute carbon is limited by the return of the yield point and deterioration in ductility, which is detrimental for formability. Generally, nitrogen is tied by addition Al and/or Ti, and the concentration of excess solute carbon is limited to about 25 wt.ppm to avoid strain aging at room temperature during storage or transportation of the steel [2,3]. The bake hardening effect is evaluated by the BH value, which is defined as the difference between the yield strength after baking and the flow stress at the end of prestraining.

A variety of metallurgical factors, for example, the concentrations of carbon, nitrogen and other alloying elements, grain size, coiling temperature, skin pass elongation, percentage prestraining, etc. strongly affect the bake hardening. In the past two decades, many researchers reported their achievements related to the development of BH steels. Hoggan and Mu Sung [3] provided the best range from 10 to 45 wt. ppm of excess solute carbon concentration to obtain the optimum BH properties. Van Snick et al. [4] investigated an ultra-low carbon (ULC) steel and found that the Nb/C ratio of 0.6-0.8 results in the higher BH value of 45 MPa, and that the coiling temperature in the range from 620 to 720°C had no clear influence on bake hardening. They found the prestraining of

* SCHOOL OF MATERIALS AND METALLURGY, UNIVERSITY OF SCIENCE AND TECHNOLOGY LIAONING, LIAONING ANSHAN, CHINA 114051
** STATE KEY LABORATORY OF ROLLING TECHNOLOGY AND ROLLING AUTOMATION,LIAONING, SHENYANG, CHINA 110000
*** IRON AND STEEL RESEARCH INSTITUTE OF ANGANG GROUP, LIAONING, ANSHAN, CHINA 114009
# Corresponding author: liweijuan826@163.com

1-2% could give a better BH value, and extending the holding time at the bake temperature could shift the curve of BH value vs. prestraining to a lower percentage [4]. Taylor et al. [5] developed a new process to control the solute carbon content to meet the requirements of bake hardening in a vanadium alloyed low carbon steel. Pechler et al. [6] confirmed that the ULC bake-hardening (ULC-BH) steel shows significantly better mechanical properties than the low carbon (LC) bake hardening steel. Scientists [7-14] studied the dissolution and precipitation of carbides in the steels during the annealing cycle using the internal friction technique. Pan and Hosbons [13] provided a comprehensive description on the determination of the concentration of solute carbon and nitrogen in ferrite, and the evaluation method of strain aging susceptibility in low carbon steels. De and De Cooman et al. [15-17] studied the effect of prestraining on bake hardening in ULC steel and the effect of Al coating, and found the AlN diffusion barrier at the coating-substrate interface, and the coating Al can act as a trap for free nitrogen and reduce the strain aging susceptibility. The Angang Group and the Boagang Group, in China, have produced various bake hardening steels, and the National Standard of China GB-T24174-2009 was issued to define the determination method of the BH value. Many investigations were devoted to study the effect of various metallurgical factors on the bake hardening. Fu et al. [18] pointed out that a prestraining of 2% results in the best BH value of 60 MPa in the experimental TRIP steel. For the bake hardening steel, the aim is to obtain suitable concentration of solute carbon atoms so that substantial strengthening occurs at the paint bake temperature providing that no strain aging occurs at room temperature.

The primary mechanisms of strengthening in low carbon steels consist of cold-work hardening, solid solution hardening, precipitation hardening, and grain boundary hardening. The solid solution hardening includes hardening induced by the formation of Cottrell atmosphere [19-27]. Jung et al. [27] investigated various mechanisms of strengthening in bake hardening steels using the impulse internal friction technique. It was confirmed that in the paint baking stage, the solute carbon atoms migrated to dislocations and formed Cottrell atmosphere, which effectively hindered kink formation and migration at the dislocations, i.e., the dislocation motion was hampered, and, thus the steel was hardened.

The effect of grain size and segregation of solute atoms to grain boundaries on bake hardening is complex. Usually, the BH value increases with the reduction in grain size [2,21,28] because the diffusion distance of carbon atoms to grain boundaries is much longer than that to dislocations, but other workers [24,29,30] pointed out that the grain size has a slight effect on bake hardening. Soenen et al. [29] reported that carbon segregated to grain boundaries during continuous annealing. Zhao et al. [24] reported that the segregation of carbon to grain boundaries on formation of Cottrell atmosphere decreases with an increase in grain size. It causes a small effect when the grain diameter is larger than 16 mm. De et al. [31] reported that, in general, the bake hardening decreases with decreasing grain size. It is reasonable to conclude that contradictory observations result from the existence of too many metallurgical factors simultaneously affecting grain boundary segregation [32] and the bake hardening phenomenon. Cui Yan et al. [33] observed that increasing grain size and improving the final cooling rate can improve the bake hardening property due to decreasing the segregation of carbon atoms at grain boundaries. Finally, it should be emphasized that Dong et al. [34] reported recently, based on three-dimensional atom probe (3DAP), that for a given carbon content (12-44 ppm), the grain interior carbon concentration increases as the grain size increases. Thus, Dong and co-workers provided, for the first time, direct experimental evidence of the diffusion of grain boundary carbon to grain interior during aging.

In this study, the bake hardening is evaluated for coarse grain experimental low carbon steel in order to analyze a relationship between the BH value and internal friction peaks, that is, the dislocation-enhanced Snoek peak and Snoek-Köster peak. The internal friction is measured using subresonant technique in an inverted torsion pendulum [7-12,14,35].

2. Snoek peak, dislocation-enhanced Snoek peak and Snoek-Köster peak in iron

The internal friction is unique technique to detect and evaluate the concentration of foreign interstitial atoms dissolved in body-centered cubic (bcc) metals and alloys [7-14,36-41]. Although it is well known that the height of carbon Snoek peak in ferritic steels is proportional to the concentration of solute atoms a careful examination of experimental internal friction curves is required. Magalas et al. [42] clearly demonstrated the effect of texture on carbon Snoek peak in a commercial rolled steel. This observation was experimentally confirmed later by other workers [43-46] and by first principle calculation, kinetic Monte Carlo and molecular dynamics simulation [47-50].

Plastic deformation in iron containing low concentration of solute atoms induces the dislocation-enhanced Snoek peak [51] or equivalently the dislocation-enhanced Snoek effect (DESE) [52], which occurs exactly at the same temperature as Snoek peak [51-58]. The dislocation-enhanced Snoek peak indicates the presence of Snoek atmosphere in the vicinity of geometrical kinks on fresh non-screw dislocation segments [51-53,57,58]. Dislocation-enhanced Snoek peak was discovered by Magalas et al. [51]. The existence of the dislocation-enhanced Snoek peak was confirmed in high-purity Fe-C alloys in 2006 [58] in resonant low-frequency internal friction measurements [7-9,35,59-63,88-90] and by De Cooman and co-workers using the resonant impulse excitation internal friction technique operating at higher frequencies [27,64-68]. The presence of the dislocation-enhanced Snoek peak and Snoek-Köster peak was also reported by Jung et al. [27] in commercial ultra-low carbon bake-hardenable steels.

It is worth mentioning that Won Seok Choi et al. [68] reported the presence of the dislocation-enhanced Snoek peak in ultra-high strength press-hardened 22MnB5 steel containing a lath martensitic microstructure. The dislocation-enhanced Snoek peak was reduced by paint baking and enhanced after additional plastic deformation performed after paint baking. Thus, the dislocation-enhanced Snoek peak was also observed in samples containing athermal martensite, the isothermal product and lower bainite in low carbon steel isothermally transformed in the M_s to M_f temperature range [64,65].

The Snoek-Köster (cold-work) peak [57,71,74,76] is caused by dragging of Cottrell atmosphere by dislocations [69-77]. A number of excellent reviews exists and the reader is referred to these for background [56,71-76]. The peak temperature of Snoek-Köster relaxation depends on concentration of solute atoms bound in the atmosphere while the relaxation strength is determined by the dislocation density. The analysis of secondary features of Snoek-Köster relaxation such as the broadening of the peak and its symmetry is outside the scope of this work.

3. Experiments

A cold rolled low carbon steel sheet, with the compositions of 0.21 C, 0.01 Si, 0.21 Mn, 0.011 P, 0.007 S, 0.019 Al, 0.002 N in wt.% was used in the present study. The microstructure of the experimental aluminium killed steel is shown in Fig. 1. The average grain size was around 160 mm. The specimens for the standard tensile test with a 20 mm gauge length were prepared along the rolling direction using an EDM machining. Tensile tests to obtain a significant range of prestrains at room temperature, i.e., 2%, 3%, 5%, 7%, and 10% were carried out using an UTM5305 universal tensile testing machine with a constant strain rate of 5 mm/min. To simulate the bake hardening treatment, the prestrained specimens were baked in a bake oven of type 101-1 at 170°C for 20 min. The BH values of the baked specimens were determined according to the National Standard of China GB/T24174-2009 by taking the average of 5 samples. The dislocation structure was investigated in a JEM-2100 transmission electron microscope (TEM). The internal friction measurements were carried out using a MFP-1000 multifunction internal friction apparatus supplied by the Institute of Solid State Physics, Chinese Academy of Sciences in Hefei [91]. Internal friction samples with dimensions of $50 \times 2 \times 1 mm^3$ were prepared from longer tensile specimens with a 50 mm gauge length. Internal friction was measured in forced oscillations at four different frequencies: 0.5 Hz, 1 Hz, 2 Hz, and 4 Hz during heating from room temperature to 650 K with a heating rate of 3 K/min and a maximum strain amplitude of 20×10^{-6}. An external magnetic field was not applied.
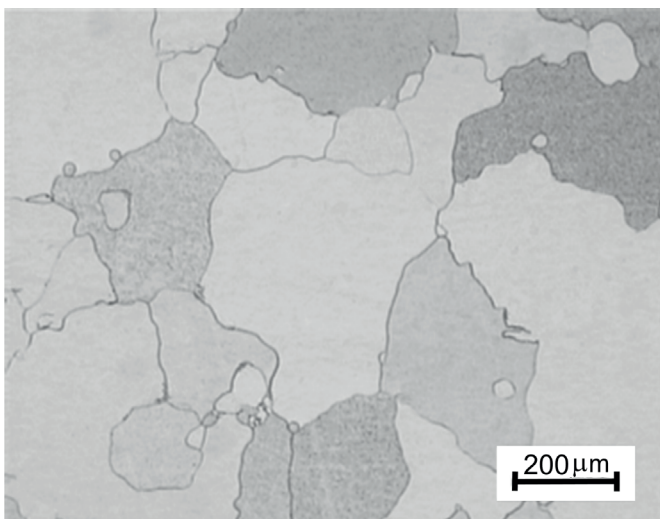

Fig. 1. The microstructure of the experimental steel observed by light microscopy

4. Experimental results

4.1. Effect of prestrain on bake hardening

Figure 2 illustrates the relationship between the BH value and the amount of prestrain at room temperature. The BH values for all the specimens turned to be smaller than zero. This is why the experimental coarse grained low carbon steel is not qualified for a bake hardenable steel. It is suggested that negative BH values are brought about due to too high annealing temperature used in the experimental steel. The BH value increases, however, with increasing prestrain from 2 to 5% firstly, and then the BH value decreases with increasing prestrain from 5 to 10%. The 5% prestrain induces the highest BH value. Thus, the bake hardening property as a function of prestrain is not monotonic. This result is consistent with the previous report [4]. However, Van Snick et al. [4] obtained the best BH value at about 2% prestrain or less. Many experimental and industrial factors affect the relationship between the BH value and prestrain [3,4]. It should be emphasized that the prestrain of 5% obtained in the present study (Fig. 2) is valid for the investigated experimental coarse grained low carbon steel.
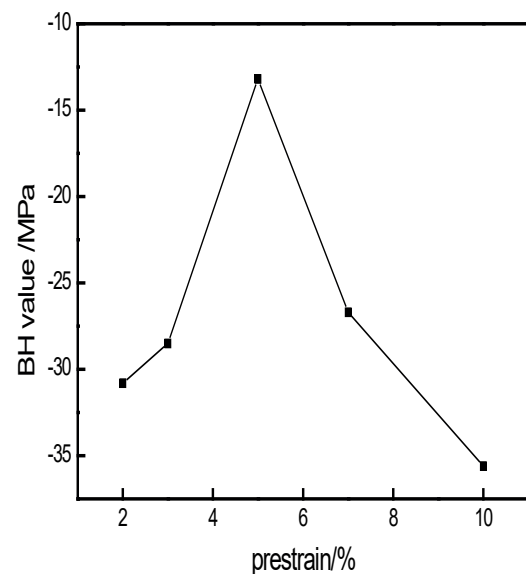

Fig. 2. The relationship between the BH value and prestrain

4.2. Effect of prestrain on dislocation density

Figure 3 shows the dislocation structure in samples subjected to different prestrain followed by the same baking treatment at 170°C for 20 min. The dislocation structure is non-uniform, with typical dislocation entanglements readily visible in the baked sample subjected to 2% prestrain (Fig. 3(a)). In the baked specimen subjected to 5% prestrain, a large amount of tangled dislocations is observed, which construct a typical dislocation network (Fig. 3(b)). In the third baked specimen subjected to 10%

prestrain, dislocation distribution is relatively uniform and the dislocation cell structure is clearly visible (Fig. 3(c)). Even though the area between cell walls suggests a lower dislocation density, the dislocation density within the cell walls must be very high, albeit difficult to resolve. No direct measurement of the dislocation density was carried out in the present work. Nonetheless Fig. 3 indicates that dislocation density increases with increasing prestrain from 2 to 5%, then the dislocation density reach a saturation stage in specimens subjected to prestrain range from 5 to 10%. Jung et al. [27] determined the dislocation density as a function of prestraining from 5 to 20% using electric resistivity, and observed a monotonic relationship and the final saturation in an experimental ULC-BH steel (see Fig. 12 in [27]).
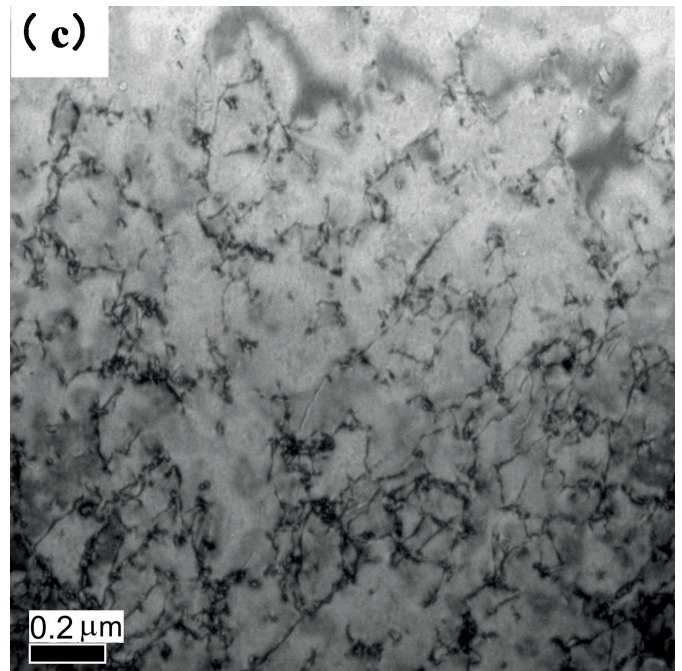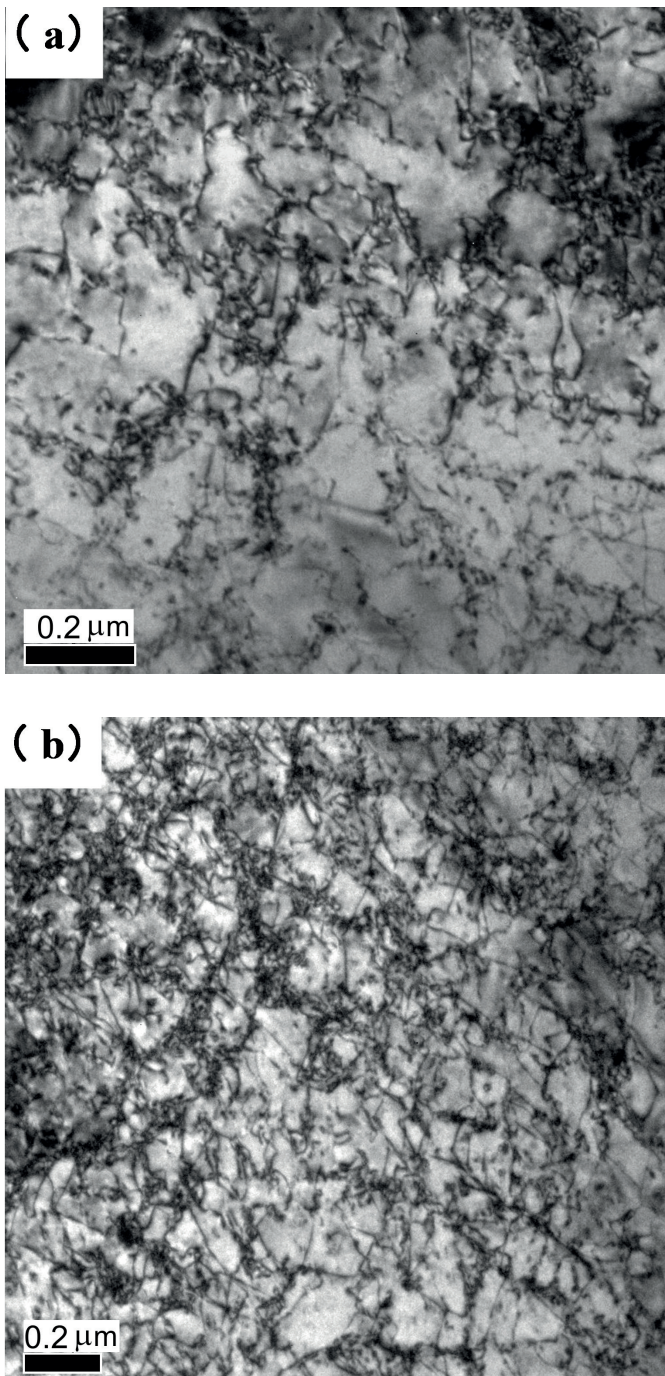

Fig. 3. Influence of prestrain on the dislocation structure in cold rolled low carbon steel after baking at 170°C for 20 min. (a) 2%, (b) 5%, and (c) 10%

4.3. The internal friction peaks after prestrain and paint baking

Figure 4 shows internal friction spectra obtained after 2%, 5% and 10% prestrain (Figs. 4a-c) and then baked at 170°C for 20 min (Figs. 4d-f). The internal friction spectra are comprised of: (1) carbon Snoek peak [7,36-41], (2) the dislocation-enhanced Snoek peak [27,51-58,64-68], and (3) Snoek-Köster peak [69-77], and typical exponential high-temperature background [70,75-77]. Resolved internal friction peaks, obtained after background subtraction, are illustrated in Fig. 5. The height of Snoek peak decreases with increasing the amount of prestrain. This result is consistent with the results reported by Jung [27] in ULC-BH steel (see Fig. 9 in [27]). It should be emphasized, however, that the experimental results reported by Jung show large dispersion in internal friction data estimated from free decaying oscillations. Such a high dispersion in internal friction is a characteristic feature of the impulse internal friction technique for high values of internal friction [27,67].

The bake hardening treatment increases the height of Snoek-Köster peak in all three specimens. The biggest increase in Snoek-Köster peak heights is observed in the specimen subjected to 5% prestrain. The result does not agree with Jung's result [27] in ULC-BH steel for pre-deforming from 0 to 10% (see Fig. 7 in [27]), where the height of Snoek-Köster peak monotonously increases with increasing the amount of prestrain. In the specimen subjected to 2% prestrain, the height of carbon Snoek peak and Snoek-Köster peak is substantially increased by bake hardening treatment. In two other specimens, only an increase in the height of Snoek-Köster peak is observed.
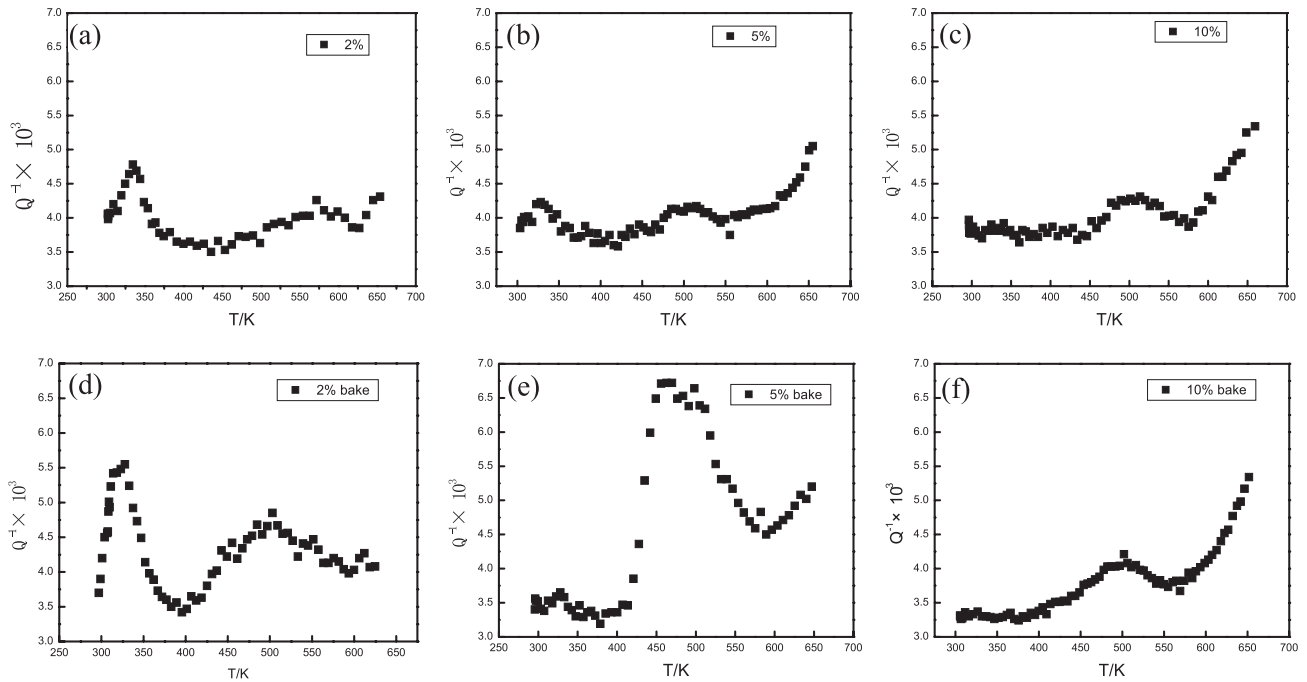
Fig. 4. Internal friction spectra measured in three specimens after different prestrains of (a) 2%, (b) 5%, (c) 10% followed by baking at 170°C for 20 min (d) 2%, (e) 5%, (f) 10%. The resonant frequency, $f_o \approx 1$ Hz
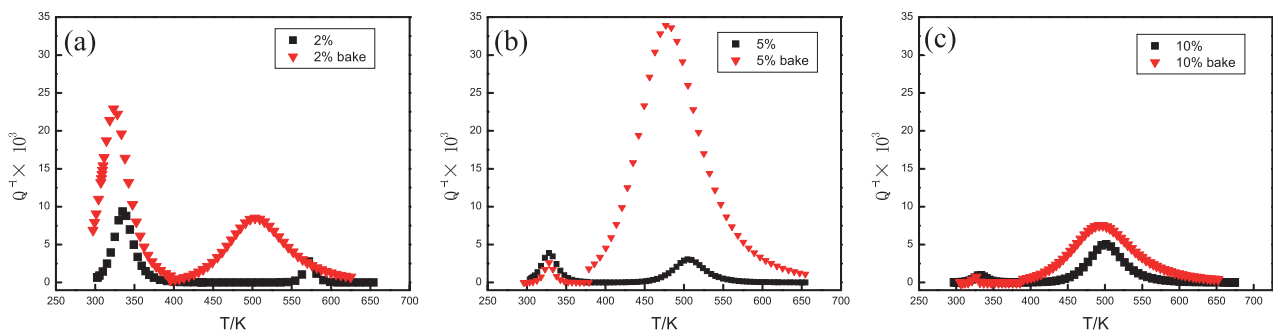

Fig. 5. Internal friction spectra from Fig. 4 after background subtraction. The samples were subjected to different prestraining: (a) 2%, (b) 5%, and (c) 10% (black curves) followed by the same baking treatment (red curves). The resonant frequency, $f_o \approx 1$ Hz

5. Discussion

It was shown [2,4] that there is a threshold value of excess solute carbon content, below which no bake hardening occurs in steels. Hoggan et al. [4] determined the threshold value C* to be approximately 10 wt.ppm in Al killed LC steel and Ti stabilized ULC steel. In this work, the BH values in coarse grain low carbon steel are negative. It implies that in the investigated coarse grained experimental steel, the concentration of dissolved carbon in solid solution of ferrite participating in the formation of Cottrell clouds must have been too low. No internal friction test was carried out for the as-received specimen, but it is believed the carbon Snoek peak in the as-received specimen was low. The heights of Snoek-Köster peaks in prestrained specimens are similar. It seems likely that the most of dissolved carbon atoms do not remain in interstitial sites of solid solution and do not segregate at dislocations but presumably segregate at grain boundaries and/or at tiny transition carbide precipitations. It should be mentioned that previous experiments [4] confirmed that the excess carbon atoms segregated to grain boundaries

do not contribute to the bake hardening effect. This is why the bake hardening is not observed the investigated coarse grained experimental steel.

The bake hardening depends on numerous parameters and a great variety of industrial variables. The interaction between the substitutional and interstitial atoms in ferrite and austenite affects the behavior of carbon atoms [79-87]. The interaction of substitutional atoms in solution with carbon atoms also affects bake hardening. Manganese exhibits an attractive interaction on the surrounding carbon atoms, especially at the first neighboring position [87]. Consequently, manganese reduces Snoek peak height [83] and limits the ability of solute carbon atoms to participate in bake hardening. Vasilyev [85] suggested that manganese may provide additional amount of carbon atoms susceptible for dislocation pinning after thermally activated dissociation of C-Mn complexes. Thus, manganese prevents participation of carbon atoms in the first stage of bake hardening.

In the present work, the baking treatment of 2% prestrained specimens transforms carbon Snoek peak into the dislocation-

enhanced Snoek peak and/or a mixture of Snoek and the dislocation-enhanced Snoek [52,54] (Figs. 4a, 4d, 5a). In the 5% prestrained specimens the dislocation-enhanced Snoek peak is less pronounced (Fig. 4b). In contrast, a substantial increase in the height of the Snoek-Köster peak is observed (Figs. 4e, 5b). The increase in the height of the Snoek-Köster peak stems from an increase in dislocation density observed in TEM (Fig. 3). The peak temperature of carbon Snoek and the dislocation-enhanced Snoek peaks remains nearly the same [27,51-54,58]. In this study, the apparent peak temperature of the dislocation-enhanced Snoek peak is slightly affected by small differences in the frequency of oscillations and variation in internal friction background.

It should be mentioned that the height of Snoek peaks measured in samples cut parallel to the rolling direction (RD) is sensitive to the fluctuation of texture components [42]. In this work, the samples were cut at 0° to the RD, which explains the variation of the height of Snoek peaks. The height of Snoek peaks remains constant for samples cut at 45° to the RD [42].

The relaxation strength of Snoek-Köster peak is associated with the dislocation density and amount of solute carbon atoms segregating to dislocations [57,69-77]. The mobility of carbon atoms bound in Cottrell atmosphere is slow down, that is, a slower diffusion of carbon atoms [75-78] is expected in Cottrell clouds. The dislocations blocked by Cottrell atmosphere are less mobile, which leads to an increase in the strength of the steel [22]. Figure 5(b) illustrates that the height of Snoek-Köster peak is substantially increased in the specimen subjected to 5% prestrain followed by bake treatment. This is why the greatest strengthening due to Cottrell atmosphere appears in the 5% prestrain specimen, and thus, the strongest bake hardening effect occurs in samples subjected to 5% prestrain. Figure 2 illustrates that this observation is in excellent agreement with the maximum BH value corresponding to 5% prestrain.

Figure 5(c) illustrates that the heights of Snoek and Snoek-Köster peaks due to the bake treatment of the specimen subjected to 10% prestrain are the lowest among the three specimens. Thus, the effect of strengthening in the 10% prestrain specimen is the lowest as confirmed by the lowest value of the BH value (Fig. 2). To conclude, it is clearly demonstrated that the BH value and Snoek-Köster peak are closely related, and the bake hardenability can be related to the height of Snoek-Köster peak. The dislocation-enhanced Snoek peak and Snoek-Köster peak can be used to detect fresh mobile dislocations pinned by Snoek atmosphere and dislocations blocked by Cottrell atmosphere at different production stages of BH steels.

It should be mentioned that the shape of internal friction peaks observed in samples subjected to prestrain of: 2%, 5% and 10% are slightly biased by the time-dependent variation of the center of oscillations during internal friction measurements [35,61-63,88-90]. Thus, it is not surprising that under such difficult experimental conditions the activation energy of the dislocation-enhanced Snoek peak was not determined in this work.

6. Conclusions

The bake hardening property (the BH value) of coarse grain experimental low carbon steel has negative values. The BH value increases, however, with an increase in prestrain from 2 to 5%, and then the BH value decreases with the increase in prestrain from 5 to 10%. In the specimen with prestrain of 5%, the BH value reaches the maximum value. The variation of the BH value with prestrain is in excellent agreement with the variation of the height of Snoek-Köster peak. The heighest Snoek-Köster peak is observed in samples subjected to 5% prestrain followed by bake treatment at 170°C for 20 min. Internal friction spectra of coarse grain experimental low carbon steel subjected to 2% prestrain and bake treatment reveal the presence of the dislocation-enhanced Snoek peak and broad Snoek-Köster peak. It is demonstrated that Cottrell atmosphere is responsible for the bake hardening even in the case of coarse grain low carbon steel. It is concluded that the dislocation-enhanced Snoek peak and Snoek-Köster peak can be used to probe the state of fresh dislocations pinned by Snoek and Cottrell atmospheres at different production stages of automotive parts. The relaxation strength of Snoek-Köster peak is closely related to the BH value.

REFERENCES

[1] E.C. Oren, Automotive materials and technology for 21st century, 39th Mechanical Working and Steel Processing Conference Proceedings, Iron & Steel Society, Warrendale, PA, USA, 639-643 (1997).

[2] R.P. Foley, M.E. Fine, S.K. Bhat, Bake hardening steels: Toward improved formability and strength, ibid., 653-666 (1997).

[3] E. Hoggan, G. Mu Sung, Cold rolled batch annealed bake hardening steel for automotive industry, ibid., 17-29 (1997).

[4] A. Van Snick, D. Vanderschuren, S. Vandeputte, J. Dilewijns, Influence of carbon and coiling temperature on hot and cold rolled properties of bake hardenable Nb-ULC steels, ibid., 225-232 (1997).

[5] K.A. Taylor, J.G. Speer, Development of vanadium-alloyed, bake hardenable sheet steels for hot-dip coated applications, ibid., 49-61 (1997).

[6] A. Pichler, H. Spindler, T. Kurz, R. Mandyczewsky, M. Pimminger, P. Stiaszny, Hot-dip galvanized bake hardening grades, a comparison between LC and ULC concepts, ibid., 63-81 (1997).

[7] A.S. Nowick, B.S. Berry, Anelastic Relaxation in Crystalline Solids, Academic Press, New York (1972).

[8] R. De Batist, Internal Friction of Structural Defects in Crystalline Solids, North-Holland, Amsterdam, 1972.

[9] L.B. Magalas, Mechanical spectroscopy – Fundamentals, Sol. St. Phen. **89**, 1-22 (2003).

[10] S. Etienne, S. Elkoun, L. David, L.B. Magalas, Mechanical spectroscopy and other relaxation spectroscopies, Sol. St. Phen. **89**, 31-66 (2003).

[11] R. Schaller, G. Fantozzi, G. Gremaud (Eds.) Mechanical Spectroscopy Q-1 2001, Mat. Science Forum **366-368** (2001).

[12] L.B. Magalas, Mechanical spectroscopy, internal friction and ultrasonic attenuation. Collection of works, Mater. Sci. Eng. A **521-522**, 405-415 (2009).

[13] Z.L. Pan, R.R. Hosbons, Determination of interstitial carbon and nitrogen in low carbon steels, 39th Mechanical Working and Steel Processing Conference Proceedings, Iron and Steel Society, Warrendale, PA, USA, **241-254** (1997).

[14] L.J. Baker, J.D. Parker, S.R. Daniel, Mechanism of bake hardening in ultralow carbon steel containing niobium and titanium additions, Materials Science and Technology **18**, 541-547 (2002).

[15] B.C. De Cooman, H. Dillen, H. Storms, I. Bultinck, P. Buysse, I.G. Ritchie, M. Kuhn, M. Fiorucci, N ageing in aluminized steel sheet: an industrial application of high frequency internal friction measurements to point defect-interface interactions, J. Alloy Compd. **211/212**, 619-624 (1994).

[16] A.K. De, S. Vandeputte, B.C. De Cooman, Static strain aging behavior of ultra-low carbon bake hardening steel, Scripta Materialia **41**, 831-837 (1999).

[17] A.K. De, K. De Blauwe, S. Vandeputte, B.C. De Cooman, Effect of dislocation density on the low temperature aging behavior of an ultra low carbon bake hardening steel, J. Alloy Compd. **310**, 405-410 (2000).

[18] R. Fu, Y. Su, P. Ye, X. Wei, L. Li, J. Zhang, Internal friction on the bake-hardening behavior of 0.11C-1.67Mn-1.19Si TRIP steel, J. Mater. Sci. Technol. **25**, 141-144 (2009).

[19] A.H. Cottrell, B.A. Bilby, Dislocation theory of yielding and strain ageing in iron, Proc. Phys. Soc. **62A**, 49-62 (1949).

[20] R.W. Cahn, P. Haasen, Physical Metallurgy, 3ed., North-Holland Physics Publishing, Amsterdam, Part II, Chapter 16, Chapter 19 and Chapter 21 (1983).

[21] P. Elsen, H.P. Hougardy, On the mechanism of bake-hardening, Steel Research **64**, 431-436 (1993).

[22] D.V. Wilson, B. Russell, The contribution of atmosphere locking to the strain-ageing of low carbon steels, Acta Metallurgica **8**, 36-45 (1960).

[23] J.Z. Zhao, A.K. De, B.C. De Cooman, A model for the Cottrell atmosphere formation during aging of ultra low carbon bake hardening steels, ISIJ International **40**, 725-730 (2000).

[24] J.Z. Zhao, A.K. De, B.C. De Cooman, Formation of the Cottrell atmosphere during strain aging of bake-hardenable steels, Metallurgical and Materials Transactions, **A33**, 417-423 (2001).

[25] J.Z. Zhao, A.K. De, B.C. De Cooman, Kinetics of Cottrell atmosphere formation during strain aging of ultra-low carbon steels, Materials Letters **44**, 374-378 (2000).

[26] A.D. De, S. Vandeputte, B.C. De Cooman, Kinetics of strain aging in bake hardening ultra low carbon steel - a comparison with low carbon steel, Journal of Materials Engineering and Performance **10**, 567-575 (2001).

[27] Il-Chan Jung, D.G. Kang, B.C. De Cooman, Impulse excitation internal friction study of dislocation and point defect interactions in ultra-low carbon bake-hardenable steel, Metall. Mater. Trans. **45A**, 1963-1978 (2013).

[28] J. Takahashi, M. Sugiyama, N. Maruyama, Quantitative observation of grain boundary carbon segregation in bake-hardening steels, Nippon Steel Technical Report **91**, 28-33 (2005).

[29] B. Soenen, A.K. De, S. Vandeputte, B.C. De Cooman, Competition between grain boundary segregation and Cottrell atmosphere formation during static strain aging in ultra-low carbon bake hardening steels, Acta Materialia 52, 3483-3492 (2004).

[30] Ch.F. Kuang, J. Wang, J. Li, S.G. Zhang, H.F. Liu, H.L. Yang, Effect of continuous annealing on microstructure and bake hardening behavior of low carbon steel, Journal of Iron and Steel Research International **22**, 163-170 (2015).

[31] A.K. De, S. Vandeputte, B. Soenen, B.C. De Cooman, Effect of grain size on the static strain aging of a ULC-bake hardening steel, Z. Metallkunde, **95**, 713-717 (2004).

[32] Xu Tingdong, Cheng Buyuan, Kinetics of non-equilibrium grain-boundary segregation, Progress in Materials Science **49**, 109-208 (2004).

[33] Cui Yan, Ji Aimin, Feng YunLi, Wang Ruizhen, Yong Qilong, Effect of grain size and annealing condition on grain boundary segregation of carbon atoms in ULC steel, Applied Mechanics and Materials **302**, 286-291 (2013).

[34] Jiling Dong, Yinsheng He, Chan-Gyu Lee, Byungho Lee, Jeongbong Yoon, Keesam Shin, Detection and determination of solute carbon in grain interior to correlate with the overall carbon content and grain size in ultra-low-carbon steel, Microsc. Microanal. **19**, S5, 66-68 (2013).

[35] L.B. Magalas, Development of high-resolution mechanical spectroscopy, HRMS: status and perspectives. HRMS coupled with a laser dilatometer, Arch. Metall. Mater. **60**, 2069-2076 (2015).

[36] J.L. Snoek, Effect of small quantities of carbon and nitrogen on the elastic and plastic properties of iron, Physica **8**, 711-733 (1941).

[37] M. Koiwa, A note on Dr. J.L. Snoek, Mat. Sci. Eng. **A 370**, 9-11 (2004).

[38] M. Weller, Anelastic relaxation of point defects in cubic crystals, J. Phys. IV, **6**, 63-72 (1996).

[39] L.B. Magalas, G. Fantozzi, Mechanical spectroscopy of the carbon Snoek relaxation in ultra-high purity iron, J. Phys. IV, **6**, 151-154 (1996).

[40] M. Weller, The Snoek relaxation in bcc metals – from steel wire to meteorites, Mat. Sci. Eng. A **442**, 21-30 (2006).

[41] M. Weller, Point defect relaxations, Mat. Science Forum **366-368**, 95-137 (2001).

[42] L.B. Magalas, G. Fantozzi, J. Rubianes, T. Malinowski, Effect of texture on the Snoek relaxation in a commercial rolled steel, J. Phys. IV, **6**, 147-150 (1996).

[43] K. Eloot, J. Dilewijns, Calculation of the effect of texture on the Snoek peak height in steels, ISIJ Int. **37**, 610-614 (1997).

[44] K. Eloot, L. Kestens, J. Dilewijns, Effect of texture on the height of the Snoek peak in electrical steels, ISIJ Int. **37**, 615-622 (1997).

[45] L.J. Baker, J.D. Parker, S.R. Daniel, The use of internal friction techniques as a quality control tool in the mild steel industry, Journal of Materials Processing Technology **143**, 442-447 (2003).

[46] R.P. Krupitzer, C.J. Szczepanski, R. Gibala, Effects of preferred orientation on Snoek phenomena in commercial steels, Mat. Sci. Eng. A **521**, 43-46 (2009).

[47] D.E. Jiang, E.A. Carter, Carbon dissolution and diffusion in ferrite and austenite from first principles, Physical Rev. B **67**,214103 (2003).

1730

[48] C. Domain, C.S. Becquart, J. Foct, Ab initio study of foreign interstitial atom (C, N) interactions with intrinsic point defects in a-Fe, Physical Rev. B **69**, 144112 (2004).

[49] S. Garruchet, M.Perez, Modelling of carbon Snoek peak in ferrite: Coupling molecular dynamics and kinetic Monte-Carlo simulations, Computational Materials Science **43**, 286-292 (2008).

[50] Shifang Xiao, Fuxing Yin, Wangyu Hu, The anisotropic character of Snoek relaxation in Fe-C system: A kinetic Monte Carlo and molecular dynamics simulation, Phys. Stat. Solidi B **252**, 1382-1387 (2015).

[51] L.B. Magalas, P. Moser, I.G. Ritchie, The dislocation-enhanced Snoek peak in Fe-C alloys, Journal de Physique **44** (C9), 645-649 (1983).

[52] L.B. Magalas, S. Gorczyca, The dislocation-enhanced Snoek effect – DESE in Iron, Journal de Physique **46** (C10), 253-256 (1985).

[53] J. Rubianes, L.B. Magalas, G. Fantozzi, J. San Juan, The dislocation-enhanced Snoek effect (DESE) in high purity iron doped with different amounts of carbon, Journal de Physique **48**, 185-190 (1987).

[54] L.B. Magalas, D.H. Niblett, Dislocation relaxations in solids, Journal de Physique, **48**, (C8), 209-217 (1987).

[55] P. Palcek, S. Fogelton, Influence of the ageing and plastic deformation on temperature dependence of internal friction, Kovove Materialy, **34**, 241-248 (1996).

[56] G.V. Serzhantova, N. Ya. Matveeva, I.S. Golovin, S.A. Golovin, Effect of plastic strain on the temperature spectrum of internal friction of austenitic and ferritic steels, Metal Science and Heat Treatment **39**, 376-383 (1997).

[57] L.B. Magalas, On the interaction of dislocations with interstitial atoms in BCC metals using mechanical spectroscopy: the Cold Work (CW) peak, the Snoek-Köster (SK) peak, and the Snoek-Kê-Köster (SKK) peak. Dedicated to the memory of Professor Ting-Sui Kê, Acta Metallurgica Sinica **39**, 1145-1152 (2003).

[58] L.B. Magalas, The Snoek-Köster (SK) relaxation and dislocation-enhanced Snoek effect (DESE) in deformed iron, Sol. St. Phen. **115**, 67-72 (2006).

[59] L.B. Magalas, Determination of the logarithmic decrement in mechanical spectroscopy, Sol. St. Phen. **115**, 7-14 (2006).

[60] L.B. Magalas, T. Malinowski, Measurement techniques of the logarithmic decrement, Sol. St. Phen. **89**, 247-260 (2003).

[61] L.B. Magalas, A. Stanisławczyk, Advanced techniques for determining high and extreme high damping: OMI - A new algorithm to compute the logarithmic decrement, Key Eng. Mat. **319**, 231-240 (2006).

[62] L.B. Magalas, M. Majewski, Recent advances in determination of the logarithmic decrement and the resonant frequency in low-frequency mechanical spectroscopy, Sol. St. Phen. **137**, 15-20 (2008).

[63] L.B. Magalas, M. Majewski, Toward high-resolution mechanical spectroscopy HRMS. Logarithmic decrement, Sol. St. Phen. **184**, 467-472 (2012).

[64] Dongowi Kim, J.G. Speer, B.C. de Cooman, Isothermal transformation of a CMnSi steel below the MS temperature, Metallurgical and Materials Transactions A, **42**, 1575-1585 (2011).

[65] Dongowi Kim, Seok-Jae Lee, B.C. de Cooman, Microstructure of low C steel isothermally transformed in the MS to Mf temperature range, Metallurgical and Materials Transactions A **43**, 44967-4983 (2012).

[66] B.C. De Cooman, Influence of interstitial-dislocation interactions on the γ-relaxation and Snoek-Kê-Köster relaxation in steel, International Symposium on Steel Science, ISSS 2012, Kyoto, Japan.

[67] I. Jung, B.C. de Cooman, The IF spectrum of Fe-C-N and Fe-17%Cr-C-N alloys measured by the impulse excitation technique, Sol. St. Phen. **184**, 209-214 (2012).

[68] Won Seok Choi, Jewoong Lee, B.C. De Cooman, Internal-friction analysis of dislocation-interstitial carbon interactions in press-hardened 22MnB5 steel, Materials Science and Engineering A **639**, 439-447 (2015).

[69] G. Schoeck, Friccion interna debido a la interaction entre dislocaciones y atomos solutos, Acta Metallurgica **11**, 617-622 (1963).

[70] L.B. Magalas, J.F. Dufresne, P. Moser, The Snoek-Köster relaxation in iron, J. de Phys. **42**, 127-132 (1981).

[71] G. Schoeck, The cold work peak, Scripta Metall. **16**, 233-239 (1982).

[72] A. Seeger, The kink-pair-formation theory of the Snoek-Köster relaxation, Scripta Metall. **16**, 241-247 (1982).

[73] G. Schoeck, On the mechanism of the Snoek-Koester relaxation, Scripta Metall. **22**, 389-394 (1988).

[74] A. Seeger, A theory of the Snoek-Köster relaxation (cold-work peak) in metals, phys. stat. sol. (a) **55**, 457-468 (1979).

[75] K.L. Ngai, Y.N. Wang, L.B. Magalas, Theoretical basis and general applicability of the coupling model to relaxations in coupled systems, J. Alloy Compd. **211/212**, 327-332 (1994).

[76] L.B. Magalas, The Snoek-Köster relaxation. New insights – New paradigms, J. de Phys. IV, **6**, 163-172 (1996).

[77] L.B. Magalas, Diffusion in the Cottrell atmosphere, Defect and Diffusion Forum **194-199**, 115-120 (2001).

[78] K.L. Ngai, Relaxation and Diffusion in Complex Systems, Springer, New York, 2011.

[79] H. Numakura, M. Koiwa, The Snoek relaxation in dilute ternary alloys. A review, J. de Phys. IV **6**, 97-106 (1996).

[80] H. Numakura, Mechanical relaxation due to interstitial solutes in metals, Sol. St. Phen. **89**, 93-114 (2003).

[81] M.S. Blanter, L.B. Magalas, Strain-induced interaction of dissolved atoms and mechanical relaxation in solid solutions. A review, Sol. St. Phen. **89**, 115-139 (2003).

[82] P.T. Liu, W.W. Xing, X.Y. Cheng, D.Z. Li, Y.Y. Li, X.Q. Chen, Effects of dilute substitutional solutes on interstitial carbon in a-Fe: Interactions and associated carbon diffusion from first-principles calculations, Phys. Rev. B **90**, 024103 (2014).

[83] H. Saitoh, N. Yoshinaga, K. Ushioda, Influence of substitutional atoms on the Snoek peak of carbon in b.c.c. iron, Acta Materialia **52**, 1255-1261 (2004).

[84] Y. You, M.F. Yan, Interactions of foreign interstitial and substitutional atoms in bcc iron from ab initio calculations, Physica B **417**, 57-69 (2013).

[85] A.A. Vasilyev, Hu-Chul Lee, N.L. Kuzmin, Nature of strain aging stages in bake hardening steel for automotive application, Materials Science and Engineering A **485**, 282-289 (2008).

[86] M.S. Blanter, L.B. Magalas, Carbon-substitutional interaction in austenite, Scripta Materialia **43**, 435-440 (2000).

[87] Chong Zhang, Jie Fu, Ruihuan Li, Pengbo Zhang, Jijun Zjao, Chuang Dong, Solute/impurity diffusivities in bcc Fe: A first-principles study, Journal of Nuclear Materials **455**, 354-359 (2014).

[88] L.B. Magalas, M. Majewski, Ghost internal friction peaks, ghost asymmetrical peak broadening and narrowing. Misunderstandings, consequences and solution, Mater. Sci. Eng. A **521-522**, 384-388 (2009).

[89] L.B. Magalas, A. Piłat, The zero-point drift in resonant mechanical spectroscopy, Sol. St. Phen. **115**, 285-292 (2006).

[90] M. Majewski, A. Piłat, L.B. Magalas, Advances in Computational High-Resolution Mechanical Spectroscopy HRMS. Part 1 - Logarithmic Decrement, IOP Conf. Series: Materials Science and Engineering **31**, 012018 (2012).

[91] Z.S. Li, Q.F. Fang, S. Veprek, S.Z. Li, Torsion pendulum method to evaluate the internal friction and elastic modulus of films, Review of Scientific Instruments **74**, 2477-2480 (2003).